DOI: 10.1002/chem.201102243

Addition of Alkynes to a Gallium Bis-Amido Complex: Imitation of Transition-Metal-Based Catalytic Systems

Igor L. Fedushkin,* Alexander S. Nikipelov, Alexander G. Morozov, Alexandra A. Skatova, Anton V. Cherkasov, and Gleb A. Abakumov*[a]

Abstract: Acetylene, phenylacetylene, and alkylbutynoates add reversibly to (dpp-bian)Ga–Ga(dpp-bian) (dpp-bian = 1,2-bis[(2,6-diisopropylphenyl)-imino]acenaphthene) to give addition products [dpp-bian($R^1C{=}CR^2$)]Ga–Ga-[($R^2C{=}CR^1$)dpp-bian]. The alkyne adds across the Ga–N–C section, which results in new carbon–carbon and carbon–gallium bonds. The adducts were characterized by electron absorption, IR, and ^{1}H NMR spectroscopy and their molecular structures have been determined by single-crystal X-ray analysis. According to the X-ray data, a change in the coordination number of gallium from three [in (dpp-bian)Ga–Ga(dpp-bian)] to four (in the adducts) results in elongation of the metal–metal bond by approximately 0.13 Å. The adducts undergo a facile alkynes elimination at elevated temperatures. The equilibrium between [dpp-bian(PhC=CH)]Ga–Ga[(HC=CPh)dpp-bian] and [(dpp-bian)Ga–Ga(dpp-bian) + 2 PhC≡CH] in toluene solution was studied by ^{1}H NMR spectroscopy. The equilibrium constants at various temperatures ($298 \le T \le 323$ K) were determined, from which the thermodynamic parameters for the phenylacetylene elimination were calculated ($\Delta G° = 2.4$ kJ mol^{-1}, $\Delta H° = 46.0$ kJ mol^{-1}, $\Delta S° = 146.0$ J K^{-1}mol^{-1}). The reactivity of (dpp-bian)Ga–Ga(dpp-bian) towards alkynes permits use as a catalyst for carbon–nitrogen and carbon–carbon bond-forming reactions. The bisgallium complex was found to be a highly effective catalyst for the hydroamination of phenylacetylene with anilines. For instance, with [(dpp-bian)Ga–Ga(dpp-bian)] (2 mol %) in benzene more than 99 % conversion of $PhNH_2$ and PhC≡CH into $PhN{=}C(Ph)CH_3$ was achieved in 16 h at 90 °C. Under similar conditions, the reaction of 1-aminoanthracene with PhC≡CH catalyzed by (dpp-bian)Ga–Ga(dpp-bian) formed a carbon–carbon bond to afford 1-amino-2-(1-phenylvinyl)anthracene in 99 % yield.

Keywords: alkynes · gallium · hydroamination · hydroarylation · redox-active ligands

Introduction

1,2-Bis(arylimino)acenaphthene (bian) ligands have attracted rising attention in recent years.[1–3] Their transition-metal complexes were first reported by Elsevier and van Asselt in the early 1990s.[1] More than 1200 d-block-metal complexes with neutral bians have been reported to date, and approximately 90 of them have been studied by X-ray analysis. Numerous articles that discussed bian complexes of transition metals were published in 2010.[2] The combination of σ-donor and π-acceptor character with conformational rigidity in the bians allows preparation of transition-metal complexes that serve as catalysts in various organic reactions, especially the polymerization of olefins and dienes.[2h–l] In 2003, the unique ability of bians to act as an electron sponge was illustrated by a four-step reduction of the most useful representative in the series—1,2-bis[(2,6-diisopropylphenyl)imino]acenaphthene (dpp-bian)—with sodium.[4] However, transition-metal complexes with anionic bian ligands are limited to the recently reported chromium(II)/dpp-bian radical anion complexes.[5] In comparison with other chelating π-acceptor ligands (for example, *o*-quinones are widely used in transition-metal chemistry), the bians have a more negative reduction potential (bians $E < -1.0$ V; quinones $E > -0.6$ V vs. the saturated calomel electrode). Therefore, transition metals in their positive oxidation states are not stable to the reducing power of coordinated anionic bian ligands. In contrast, Group 1, 2, 13, and 14 metals,[6a] as well as the lanthanides,[6b] form thermodynamically stable complexes with radical-anionic and dianionic bian ligands. The main research motive in the field of main-group-metal complexes of bians is to generate redox-active complexes of redox-inactive metals, such as magnesium(II) or aluminum(III), by using redox-active bian ligands. It is expected that this type of complex may demonstrate new types of catalytic activity or emulate the catalytic behavior of known transition-metal complexes. The concept of ligands that can store and release electrons during catalytic processes has begun to

[a] Prof. Dr. I. L. Fedushkin, A. S. Nikipelov, Dr. A. G. Morozov, Dr. A. A. Skatova, A. V. Cherkasov, Prof. Dr. G. A. Abakumov
Institute of Organometallic Chemistry
Russian Academy of Sciences
Tropinina 49
603950 Nizhny Novgorod (Russia)
Fax: (+7) 831-2627-497
E-mail: igorfed@iomc.ras.ru

Supporting information for this article is available on the WWW under http://dx.doi.org/10.1002/chem.201102243.

be exploited in transition-metal chemistry. The development of this approach has just been highlighted by Dzik et al.[7]

Applications of transition-metal complexes with "standard" spectator ligands in homogeneous catalysis are ensured by two distinct features of transition-metal ions: 1) the ability to coordinate unsaturated organic molecules; 2) the ability to exist in several, easily interchangeable oxidation states. The latter makes oxidative addition and reductive elimination possible at a single transition-metal center. A lack of these features was always one of the limiting factors for the use of main-group metals in catalyses that were successfully performed with transition metals. Nevertheless, s-, p-, and f-block-metal complexes that can emulate the reactivity of transition-metal complexes have been produced. In this context, a complex of the dpp-bian dianion with magnesium, [(dpp-bian)Mg(thf)$_3$], is an illustrative example. The complex exhibits diverse reactivity towards various substrates. In the course of the reactions of [(dpp-bian)Mg(thf)$_3$] dramatic changes are noted in the electronic configuration, atomic arrangements, and functionality (bis-amido, amido-imino, amido-amino) of the dpp-bian ligand (Scheme 1).[8]

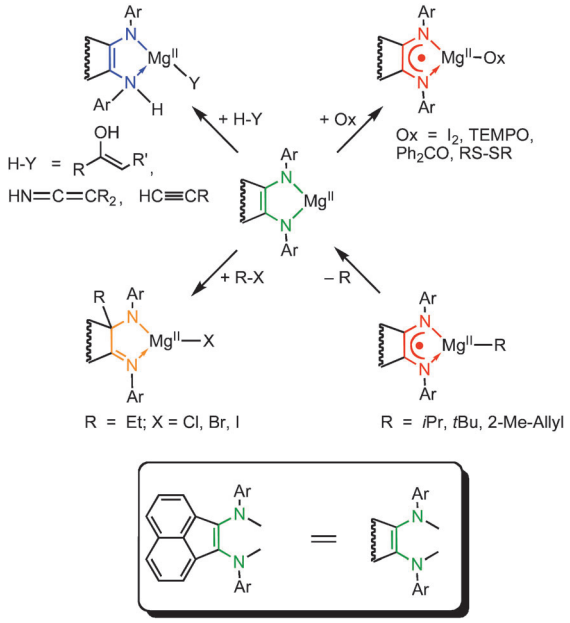

Scheme 1. Reactivity of [(dpp-bian)Mg(thf)$_3$]; coordinated solvent molecules are omitted. TEMPO = 2,2,6,6-tetramethylpiperidine *N*-oxide.

Because the reactivity of transition-metal complexes can be fine-tuned by changing the nature of the spectator ligands, variation of the metal ion at the dpp-bian dianion may change the reaction course. Switching from [(dpp-bian)Mg(thf)$_3$] to [(dpp-bian)Ga–Ga(dpp-bian)] (**1**) the pathway for reaction with phenylacetylene changes from acid–base interaction (Scheme 1) to 1,3-dipolar cycloadditions.[9] From a structural point of view, digallene **1** illustrates the influence of the conformational rigidity and electronic lability of the ligand on the molecular structure and chemical properties of the complex. Due to steric reasons, the phenyl rings at the nitrogen atoms in the dpp-bian dianion are orientated perpendicular to the metallacycle, the nitrogen atoms are forced to adopt sp^2 hybridization, and the isopropyl groups shield the nitrogen lone pairs. The three-coordinate gallium species represents a typical Lewis acid and **1** can be isolated as solvent-free complex, even from strongly coordinating solvents, such as diethyl ether or THF. Thus, a three-coordinate gallium atom in compound **1** can be considered an unsaturated center, which, in theory, could bind compact electron-rich moieties (e.g., carbon–carbon multiple bonds). This concept has been realized[9] and the data obtained are presented in this paper. We demonstrate the possibility of the binding and activation of alkyne triple bonds by gallium complex **1**, which contains a redox-active diimine ligand. We further show that alkynes bound to complex **1** become reactive towards electron-rich reagents, similar to olefins or arenes when coordinated to transition metals.

Results and Discussion

Reactions of alkynes with (dpp-bian)Ga–Ga(dpp-bian)

Characterization of complexes ***2–5***: Treatment of a solution of **1** in toluene with HC≡CH, PhC≡CH, MeC≡CCO$_2$Me, or MeC≡CCO$_2$Et at ambient temperature caused an instant color change of the solution from deep-blue to red. All four reactions proceed as [3+2] cycloadditions and afforded compounds **2–5**, respectively (Scheme 2). Digallane **1** is selective toward alkynes and does not react with other substances that contain multiple bonds, for example, H$_2$C=C(Me)CO$_2$Me, Me$_2$C=O, RC≡N (R = Me, Ph), and PhNC. Among the possible mechanisms of alkyne addition to complex **1**, a concerted process—interaction of the LUMO (π*) of the alkyne with the HOMO (π) of **1**—seems to be the most plausible. Products **2–5** were isolated as red crystals by room temperature crystallization from diethyl ether (**2**), 1,2-dimethoxyethane (**3**), or benzene (**4**, **5**). Compounds **2–5**

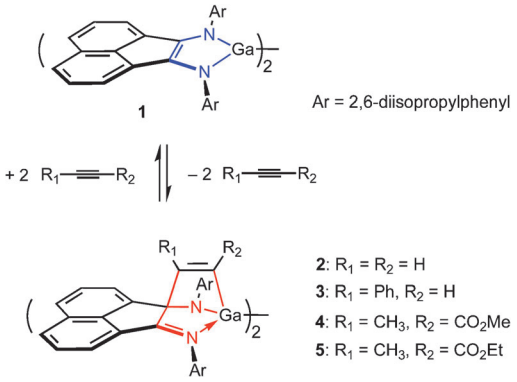

Scheme 2. Reaction of **1** with alkynes.

have been characterized by elemental analysis, IR and ^{1}H NMR spectroscopy, and X-ray crystallography.

In transition-metal chemistry there is a sole example of a related isolable compound produced from the reaction of a very strong π-acceptor alkyne ($MeO_2CC{\equiv}CCO_2Me$) with a zero-valent iron complex with N,O-chelating ligand [(*t*BuN=C(H)−C(Ph)=O)Fe(CO)(dppe)] (dppe = 1,2-bis(diphenylphosphino)ethane).[10] Frühauf and co-workers established the formation of kinetically unstable [3+2] cycloadducts in the reactions of Fe-, Ru-, and Mn complexes of 1,4-diaza-1,3-dienes (dads) with reagents that contained π-acceptor multiple carbon–carbon and carbon–element bonds.[11] The dad complexes of the transition metals are inert towards less-reactive substrates, for example, PhC≡CH and HC≡CH. Cycloaddition products related to compounds **2**–**5** have been isolated from the reaction of aromatic ketones with dad complexes of zirconium[12a] and samarium.[12b] In the same manner, iridium[13a] and rhodium[13b] catecholates add dioxygen across the metal–oxygen–carbon atom 1,3-dipole to give isolable endoperoxides. In main-group-metal chemistry the only example of a cycloaddition with reversible binding of dioxygen was found to be mediated by triphenylstibiumcatecholate and -amidophenolate complexes.[14] Note that the reactions of [(dpp-bian)Mg(thf)$_3$] with R−X (Scheme 1) also proceed by addition across the metal–ligand 1,3-dipole and result in new carbon–carbon and magnesium–halide bonds.[15] In the context of activation of carbon–carbon multiple bonds in main-group-metal complexes, the recently reported addition of $H_2C{=}CH_2$ to the metal–metal triple bond in ArSn≡SnAr is remarkable.[16a] Further, terminal alkynes can be activated by systems comprised of Lewis pairs (Scheme 3).[16b–d]

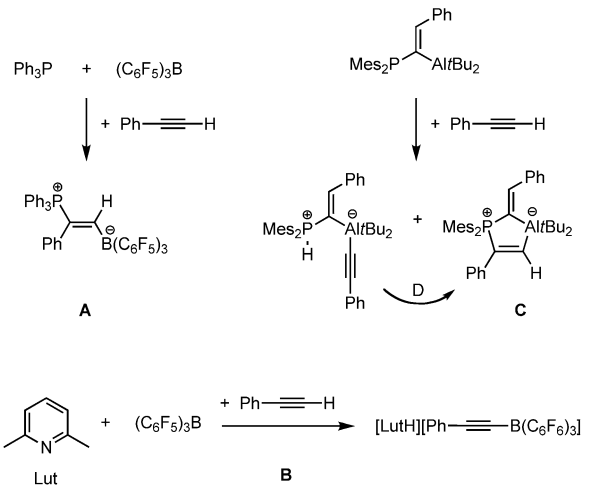

Scheme 3. Activation of phenylacetylene with Lewis pairs (**A**,[16b] **B**,[16c] and **C**[16d]).

Cycloaddition of alkynes across the Ga−N−C fragment in **1** makes one carbon atom in each metallacycle and both gallium atoms chiral, thus there are four asymmetric centers in dinuclear complexes **2**–**5**. Hence, one may expect the formation of *R*,*R*- and *S*,*S*-enantiomers, plus the *R*,*S*-diastereomers for every addition. The ^{1}H NMR spectrum of compound **2** is depicted in Figure 1 (for the ^{1}H NMR spectrum

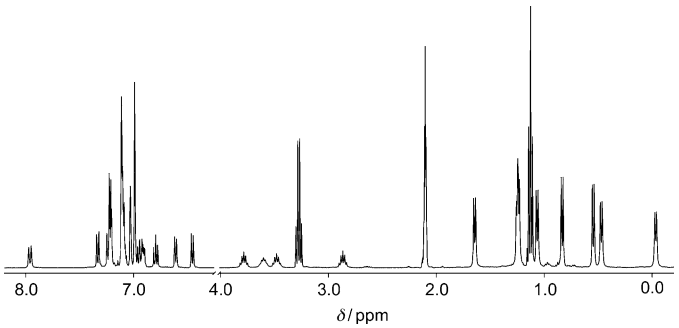

Figure 1. ^{1}H NMR spectrum of complex **2** (293 K, 400 MHz, [D$_8$]toluene).

of compound **3** see the Supporting Information). Both spectra confirm the presence of only one isomer in toluene solution. The ^{1}H NMR spectroscopic data obtained for **4** and **5** in [D$_8$]toluene (see the Supporting Information) suggest the presence of homochiral enantiomers (*R*,*R* and *S*,*S*) in solution, together with the *R*,*S*-diastereomers. These data are consistent with the results of X-ray crystallography of compounds **2**–**5** (see Figures 6–9 below). The asymmetry of the ligands in **2**–**5** causes non-equivalence of the four methine protons and eight methyl groups of the four isopropyl substituents. In complex **2**, the methine protons give rise to four septets ($\delta = 3.78$, 3.60, 3.48, and 2.87 ppm) and the methyl groups appear as eight doublet signals ($\delta = 1.64$, 1.25, 1.24, 1.06, 0.83, 0.54, 0.47, and −0.03 ppm). The low-field singlet ($\delta = 7.93$ ppm) in the ^{1}H NMR spectrum of complex **3** is assigned to the proton at the C=C double bond, which originates from the C≡C triple bond of phenylacetylene.

The IR spectra of crystalline adducts **2**–**5** were recorded in paraffin oil. The IR spectra of 2-ethylbutynoate and the product of its addition to digallane **1** are presented in the Supporting Information. The spectra of **2**–**5** reveal a strong absorption at $\tilde{\nu} = 1635 \pm 5$ cm^{-1}, which corresponds to the stretching vibrations of the carbon–nitrogen double bond. In the IR spectrum of free dpp-bian, the corresponding C=N vibrations appear in the range $\tilde{\nu} = 1642$–1670 cm^{-1}.[17] Further, in the IR spectra of **2**–**5** the absorptions related to the C≡C bond are absent. For instance, the carbon–carbon triple bond of 2-ethylbutynoate gives rise to a very strong absorption at $\tilde{\nu} = 2242$ cm^{-1}. The absorption arising from the ester group in **5** is shifted by 15 cm^{-1} to a lower wavenumber relative to free 2-ethylbutynoate ($\tilde{\nu} = 1711$ cm^{-1}). In the IR spectra of compounds **2**–**5** the carbon–carbon double bonds that result from the cleavage of one of the π bonds of the alkynes cause absorptions of medium intensity at 1585 ± 2 cm^{-1}.

*Elimination of alkynes from complexes **2**–**5***: Compounds **2** and **3** eliminate the corresponding alkyne in toluene solution at elevated temperatures. The temperature-dependent equi-

librium in the systems [**2**] ⇌ [**1** + 2 HC≡CH] and [**3**] ⇌ [**1** + 2 PhC≡CH] has been monitored by electron absorption spectroscopy. The absorption spectrum of complex **2** in toluene at different temperatures is depicted in Figure 2; the spectrum of compound **3** is provided in the Supporting Information.

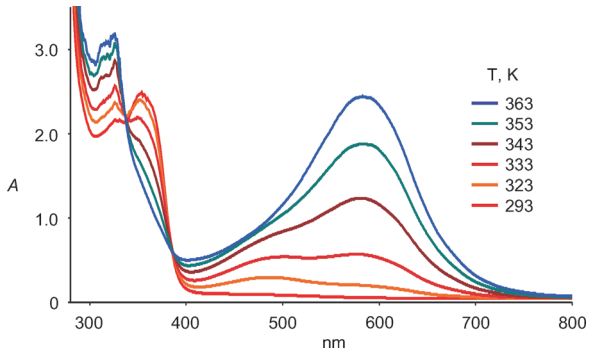

Figure 2. Temperature dependence of the absorption spectrum of complex **2** in toluene.

At 293 K the absorption maxima for **2** and **3** are located at approximately 350 nm, which corresponds to the red color of their toluene solutions. Upon raising the temperature, the intensity of this absorption gradually decreases with a concurrent increase of the absorption at 585 nm, which clearly indicates the formation of digallane **1**.[18] For the solutions of **2** and **3**, the spectral pictures remain unchanged at temperatures above 363 and 343 K, respectively, indicative of full conversion of **2** and **3** into the corresponding starting materials at those temperatures. The elimination processes are reversible; lowering the temperature to 293 K leads to restoration of the initial spectral image. However, extended heating of solutions of **2** or **3** in toluene at reflux or standing at ambient temperatures for more than one month led to conversion of the alkynes to unidentified products and the regeneration of digallane **1**, which is stable in solution for an indefinite period of time. The heating of solutions of **4** and **5** in toluene up to 373 K does not result in any visible color change of the solution. However, the electron absorption spectroscopy allows detection of weak spectral changes for a solution of **4** in toluene in the range of 293–373 K (Figure 3). In the case of **4**, the alterations of the absorption intensities are similar to those observed for solutions of **2** and **3** at ambient temperature. In all three cases, at the initial stages of the elimination processes intermediate absorption at $\lambda = 488$ nm could be detected. We assign this absorption to a species in which the alkyne has added to only one of the two metal fragments.

Because calculation of reliable equilibrium constants from the UV/Vis data obtained for **2** and **3** is difficult we decided to use ^{1}H NMR spectroscopy for determination of these constants. The upfield region of the ^{1}H NMR spectrum of complex **3** at 293 K is depicted in Figure 4a. Raising the temperature from 293 to 353 K leads to gradual replacement

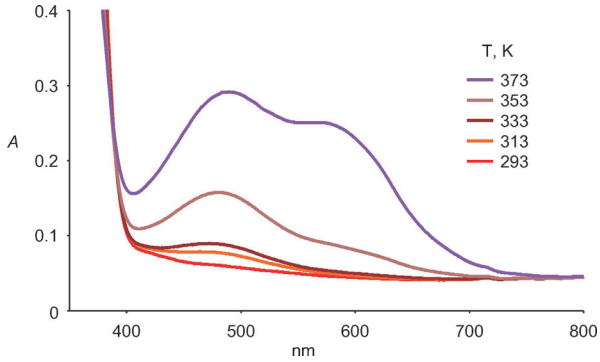

Figure 3. Temperature dependence of the absorption spectrum of complex **4** in toluene.

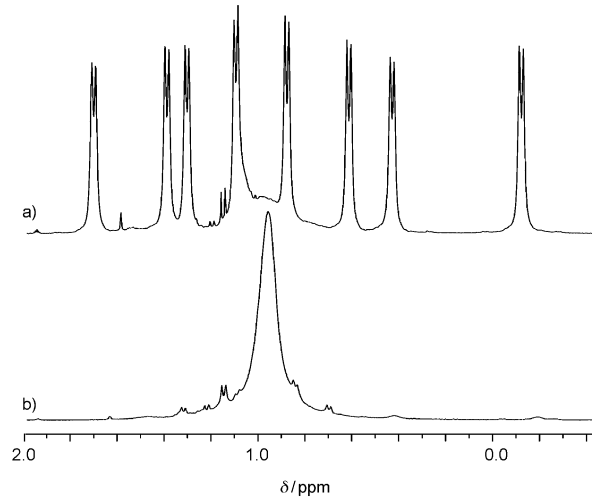

Figure 4. The upfield region of the ^{1}H NMR spectra of complex **3** in [D_8]toluene at a) 293 and b) 353 K.

of the eight doublets (each 3H) of the methyl groups in the ^{1}H NMR spectrum of complex **3** by a broadened signal (24H) centered at $\delta = 0.99$ ppm (Figure 4b). The latter is a result of coalescence of two methyl group doublets of the digallane **1**.

In the ^{1}H NMR spectrum of compound **1** at 293 K in C_6D_6 the analogous doublets (each 12H) appeared at $\delta =$ 1.01 and 0.97 ppm.[18] The intensity of the four septets (each 1H) of the methine protons of the four isopropyl groups decreased with rising temperature. In parallel, a broad signal (4H) at $\delta = 3.42$ ppm grew ($\delta \approx 3.47$ ppm for **1** in C_6D_6 at 293 K). At each temperature chosen in the range 298–323 K, an equilibrium constant (K_{eq}) could be calculated from the relative amounts of **1** and **3** at that given temperature, determined from the integrals of the methine and methyl proton resonances in the ^{1}H NMR spectra. The measured data points give a straight line when plotting the reciprocal temperature values against the natural logarithm of the equilibrium constants (see the Supporting Information). Assuming that ΔH and ΔS are constant across the temperature range 298–323 K, the thermodynamic standard parameters for the

elimination of two PhC≡CH moieties from **3** are: $\Delta G° = 2.4\ kJ\,mol^{-1}$, $\Delta H° = 46.0\ kJ\,mol^{-1}$, $\Delta S° = 146.0\ J\,K^{-1}\,mol^{-1}$). The positive value of ΔG indicates that complex **3** is thermodynamically more stable than digallane **1**. The enthalpy of the alkyne elimination for dinuclear complex **3** in toluene ($\Delta H° = 46.0\ kJ\,mol^{-1}$) is rather small if a cleavage of two carbon–carbon and two carbon–gallium bonds is assumed. To gain more insight into the alkyne elimination we investigated the solid-state behavior of complex **3**. In a sealed glass capillary, red crystals of complex **3** became dark blue when heated to 373 K. As shown by thermal gravimetric analysis (TGA), elimination of the alkyne from solid **3** begins at $T >$ 373 K (Figure 5).

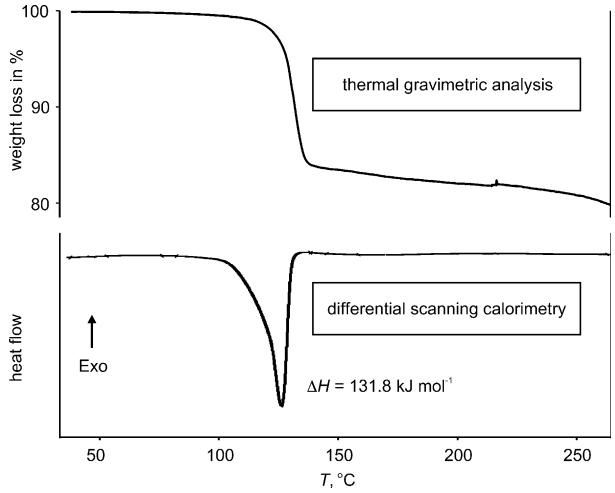

Figure 5. TGA and DSC curves for complex **3** curve.

In the temperature range 373–410 K, the crystals of **3** lose approximately 16% of their mass, which corresponds to liberation of two phenylacetylene molecules per dimeric complex **3**. Note, the temperature interval for elimination of the alkyne unit from solid **3** is much narrower (≈35 K) relative to the interval in toluene solution (≈70 K). We explain this by the different conditions of the UV-VIS experiment versus the TGA experiment. The spectroscopic measurements were carried out in a sealed glass cell, whereas the TGA experiment was conducted in a nitrogen flow that purged the eliminated alkyne. Also, according to the differential scanning calorimetry (DSC) measurements, the heat absorbed when the alkyne is eliminated from **3** in the solid state ($\Delta H° = 131.8\ kJ\,mol^{-1}$, Figure 5) is about 30% higher than in solution ($\Delta H° = 94.8\ kJ\,mol^{-1}$). This difference reflects the influence of the crystal-lattice energy on the elimination process.

*Crystal structures of complexes **2–5***: The molecular structures of compounds **2–5** were determined by X-ray crystallography at 100 K and are depicted in Figures 6–9. The crystal data and structure-refinement details are collected in Table 1. The crystal structures of **2–5** prove that, in each

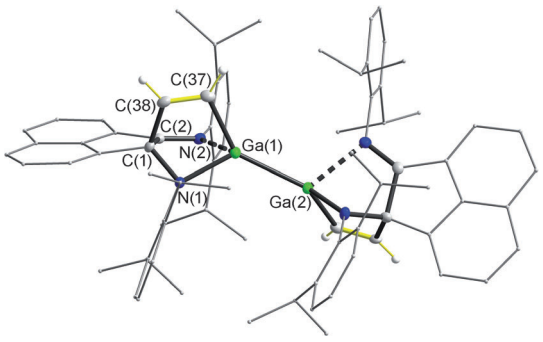

Figure 6. The molecular structure of complex **2**. Selected bond lengths [Å]: Ga(1)–Ga(2) 2.4067(4), Ga(1)–N(1) 1.929(2), Ga(1)–N(2) 2.190(2), Ga(1)–C(37) 1.994(3), N(1)–C(1) 1.481(3), N(2)–C(2) 1.280(3), C(1)–C(2) 1.550(3), C(1)–C(38) 1.551(3), C(37)–C(38) 1.316(3).

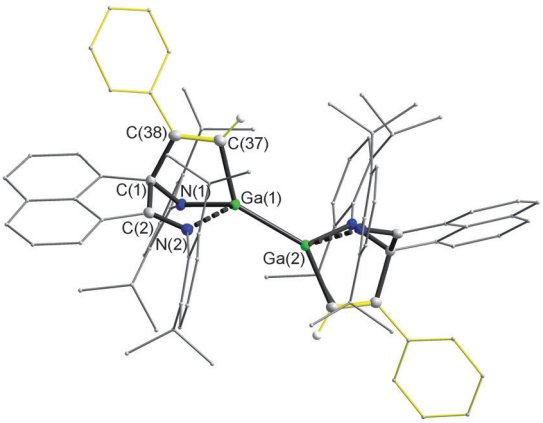

Figure 7. The molecular structure of complex **3**. Selected bond lengths [Å]: Ga(1)>C->Ga(2) 2.4052(3), Ga(1)–N(1) 1.926(1), Ga(1)–N(2) 2.173(1), Ga(1)–C(37) 1.988(1), N(1)–C(1) 1.476(2), N(2)–C(2) 1.280(2), C(1)–C(2) 1.554(2), C(1)–C(38) 1.575(2), C(37)–C(38) 1.336(2).

case, the alkyne adds across the Ga–N–C fragment to result in carbon–carbon and carbon–gallium bond formation.

Increase in the coordination number of the gallium atoms from three (**1**) to four (**2–5**) causes elongation of the Ga–Ga bond by approximately 0.05 Å relative to **1** (2.3598(3) Å).[18] The atoms C(1) and Ga(1), and their analogues in the second part of the dimer, become chiral upon the cycloaddition of alkynes. The result is four asymmetric centers in the dinuclear complexes **2–5**. In the crystals, complexes **2** and **3** are represented as C-homochiral dimers (two pairs of *R*,*R*- and *S*,*S*-enantiomers). In the case of compound **5**, the unit cell only includes a heterochiral dimer. Complex **4** represents the third case: the unit cell simultaneously consists of two pairs of *R*,*R*- and *S*,*S*-enantiomers (C-homochiral dimers) as well as the *R*,*S* diastereomer. The regioselectivity of addition of alkynes to digallane **1** is controlled by electronic rather than steric factors. Thus, in complex **3**, the bulkier Ph substituent at the C≡C triple bond is orientated away from the metal (Figure 7), whereas in the case of **4** and **5** the bulkier ester group is orientated towards the metal (Figures 8 and 9). The carbon–carbon triple bonds in

Table 1. Crystal data and structure refinement details for compounds **2**–**5**.

Compound	**2**	**3**	**4**	**5**
Formula	$C_{76}H_{84}Ga_2N_4$	$C_{88}H_{92}Ga_2N_4$·1.075 $C_4H_{10}O_2$	$C_{82}H_{92}Ga_2N_4O_4$·C_6H_6	$C_{84}H_{96}Ga_2N_4O_4$·$3C_6H_6$
M_r [g mol^{-1}]	1192.91	1441.98	1415.14	1599.47
T [K]	100	100	100	100
crystal system	monoclinic	monoclinic	monoclinic	triclinic
space group	$P21/c$	$P21/n$	$C2/c$	$P\bar{1}$
a [Å]	17.741(2)	17.3786(19)	29.176(4)	15.546(6)
b [Å]	26.137(3)	26.579(3)	12.985(2)	15.791(6)
c [Å]	13.6513(17)	17.903(2)	39.497(6)	21.274(8)
α [°]	90	90	90	70.086(7)
β [°]	89.915(3)	108.121(2)	100.678	76.781(8)
γ [°]	90	90	90	61.731(6)
V [Å^3]	6330.1(13)	7859.1(15)	14704(4)	4310(3)
Z	4	4	8	2
ρ_{calc}, [g m^{-3}]	1.252	1.219	1.279	1.232
μ [mm^{-1}]	0.898	0.737	0.788	0.680
$F(000)$	2520	3055	5984	1696
crystal size, [mm^3]	0.32×0.10×0.08	0.34×0.25×0.22	0.12×0.10×0.10	0.15×0.10×0.08
$\theta_{min}/\theta_{max}$	1.39/28	1.43/29	1.42/27	1.02/27.50
index ranges	$-23 \le h \le 23$	$-23 \le h \le 23$	$-33 \le h \le 37$	$-19 \le h \le 20$
	$-34 \le k \le 34$	$-36 \le k \le 30$	$-16 \le k \le 16$	$-19 \le k \le 20$
	$-17 \le l \le 18$	$-24 \le l \le 24$	$-50 \le l \le 50$	$0 \le l \le 27$
reflections collected	50835	73068	58589	29553
independent reflections	15272	20873	16047	19808
R_{int}	0.0812	0.0383	0.0903	0.0000
max/min transmission	0.932/0.762	0.855/0.788	0.925/0.911	0.948/0.905
data/restraints/parameters	15272/0/755	20873/3/943	16047/0/879	29554/4/1028
GOF on F^2	1.006	1.012	0.956	0.993
final R indices [$I > 2\sigma(I)$]	$R_1 = 0.0465$	$R_1 = 0.0388$	$R_1 = 0.0616$	$R_1 = 0.0883$
	$wR_2 = 0.0908$	$wR_2 = 0.0890$	$wR_2 = 0.1061$	$wR_2 = 0.1518$
R indices (all data)	$R_1 = 0.0898$	$R_1 = 0.0593$	$R_1 = 0.1475$	$R_1 = 0.2192$
	$wR_2 = 0.1059$	$wR_2 = 0.0987$	$wR_2 = 0.1355$	$wR_2 = 0.2026$
largest diff. peak/hole [e Å^{-3}]	0.539/−0.494	0.926/−0.511	0.648/−0.689	0.962/−0.843

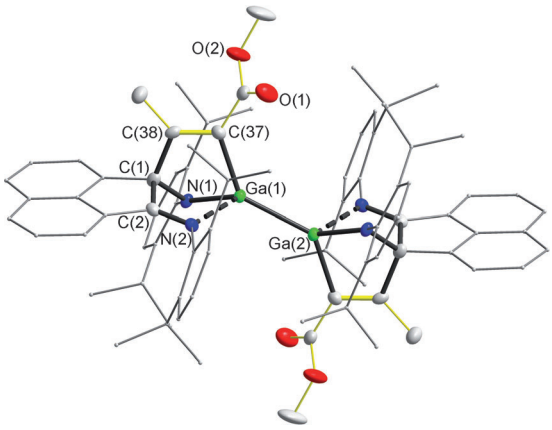

Figure 8. The molecular structure of complex **4**. Selected bond lengths [Å]: Ga(1)–Ga(2) 2.416(1), Ga(1)–N(1) 1.904(3), Ga(1)–N(2) 2.203(3), Ga(1)–C(37) 2.015(4), N(1)–C(1) 1.465(5), N(2)–C(2) 1.272(5), C(1)–C(2) 1.556(6), C(1)–C(38) 1.574(6), C(37)–C(38) 1.333(6).

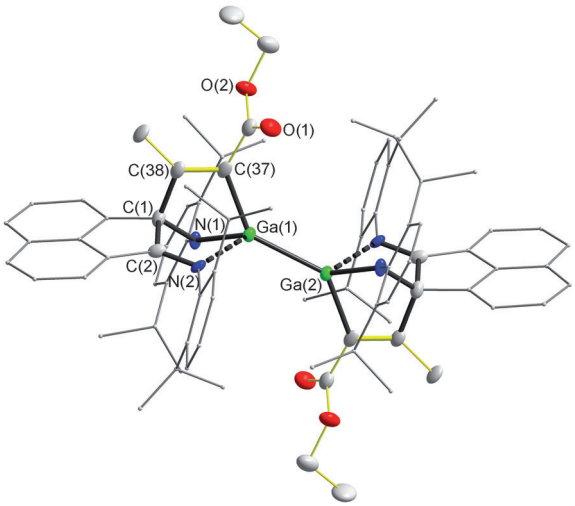

Figure 9. The molecular structure of complex **5**. Selected bond lengths [Å]: Ga(1)–Ga(2) 2.419(1), Ga(1)–N(1) 1.913(5), Ga(1)–N(2) 2.193(5), Ga(1)–C(37) 2.020(6), N(1)–C(1) 1.463(7), N(2)–C(2) 1.282(7), C(1)–C(2) 1.556(8), C(1)–C(38) 1.568(8), C(37)–C(38) 1.335(7).

alkynes PhC≡CH and MeC≡CCO$_2$R (R = Me, Et) are polarized as shown in Figure 10. Interaction of the opposite charges of the alkynes with the Ga–N–C 1,3-dipole defines the formation of the regioisomers that are observed.

A marked difference in the Ga–N bond lengths within each metallacycle in compounds **2**–**5** (Figures 6–9) reflects the amido-imino character of the N-chelating fragment. The slightly distorted trigonal planar environments of atoms C(37) and C(38) are credited to their sp^2 nature and the C(37)=C(38) bond lengths (1.316(3)–1.336(2) Å) correspond perfectly to double bonds. The newly formed C(1)–C(38) bonds (1.551(3)–1.575(2) Å) are longer than a typical single

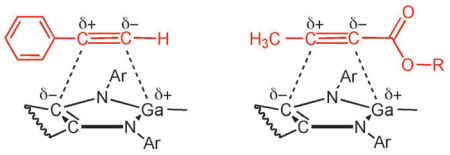

Figure 10. Regioselectivity of the alkyne addition.

C–C bond (1.54 Å). The Ga(1)–C(37) bond lengths (1.988(1)–2.020(6) Å) are comparable with those reported in gallium–vinyl derivatives $[(CH_2{=}CH)_2Ga(\mu\text{-}P(t\text{Bu})_2)]_2$ (1.95(2) and 1.96(2) Å)[19a] and 1,4-C_6H_4[HC=C($SiMe_3$)Ga-(tBu)$_2$]$_2$ (1.974(4) Å).[19b] Considering the lengths of the newly formed C–C and C–Ga bonds, the facile elimination of alkynes from **2**–**5** observed at elevated temperatures is very surprising.

Reactions of phenylacetylene with anilines catalyzed by complex 1: New carbon–nitrogen bond-forming reactions are of special interest, in both organic synthesis and industrial chemistry, because amines and their derivatives are important industrial chemicals.[20] The hydroamination of alkynes—addition of an NH unit to a carbon–carbon triple bond—is a useful method to produce new nitrogen-containing organic compounds. Among other advantages, this synthetic approach is attractive in terms of atom economy because the alkyne and amine combine to give a single product without waste. Transition-metal complexes are the most efficient catalysts for hydroamination of unsaturated substrates, such as alkenes, alkynes, allenes, and dienes.[21] Obtaining a high regioselectivity of the addition with terminal and internal asymmetric alkynes remains a problem. Chiral lanthanide complexes display high activity in enantioselective intramolecular hydroamination.[22] Also, application of non-transition-metal complexes as catalysts of hydroamination reactions has been reported. Thus, the α-diketiminate derivatives of magnesium and calcium serve well as precatalysts for the hydroamination/cyclization of aminoalkenes.[23] Roesky and co-workers have demonstrated the catalytic efficiency of pyrrolyl and aminotroponiminate calcium and zinc complexes in the intramolecular hydroamination of aminoalkenes.[24] Hydroamination reactions catalyzed by aluminum or gallium complexes have not yet been reported but their use as catalysts is attractive because these metals are readily available and nontoxic. Taking the unique reactivity of digallane **1** towards alkynes into account, assessment of the catalytic activity of **1** in hydroamination of alkynes seemed very reasonable. Catalyst complex **1** was tested in the reactions of PhC≡CH with a series of anilines. All of the reactions were performed with **1** (2 mol %) in C_6D_6 in an NMR tube. The results are summarized in Table 2. The reactions presented in Table 2, entries 2 and 9, were also carried out on a preparative scale and products **7b** and **14b** were isolated and characterized (including by X-ray crystallography).

We have found that **1** serves well as a Markovnikov-selective catalyst for the hydroamination of PhC≡CH by various anilines. Starting from anilines **6a**, **7a**, and **9a**–**11a**, the corresponding imines **6b**, **7b**, and **9b**–**11b** were obtained in high yields (Table 2, entries 1, 2, and 4–6). However, **1** does not catalyze the hydroamination of phenylacetylene with anilines that possess alkyl substituents on the aromatic ring, for example, 2,6-diisopropylphenylamine and 2,5-di-*tert*-butylphenylamine. Furthermore, the reaction rates of anilines with a substituent *ortho* to the amino group (**9a**, **10a**, and **12a**) are remarkably low relative to the rates with *meta*- or *para*-substituted anilines. These data indicate that *ortho* substituents effectively shield the aniline amino group, thus making phenylacetylene unreactive towards these anilines, even in the presence of **1**. The difference in reactivity between closely related anilines **7a** and **8a** in the reaction with phenylacetylene in the presence of catalytic **1** (Table 2, entry 2 versus 3) seemed unusual at first glance. However, a low yield of the hydroamination product **8b** can be explained by the reaction of **8a** with **1**, which proceeds through cleavage of the Br–C(aryl) bond and oxidation of the dpp-bian dianion to the radical anion. Finally, the reaction results in destruction of the catalyst.

The reaction of 1-aminonaphthalene (**13a**) with phenylacetylene catalyzed by digallane **1** gives two products in nearly equimolar quantities. The first is the Markovnikov hydroamination product **13b**, the second is the hydroarylation product **13c**, also formed according to Markovnikov's rule (Table 2, entry 8). The ^{1}H NMR spectra of the mixture of **13a** and phenylacetylene before addition of digallane **1** and of the mixture after a full conversion of the reagents in the presence of **1** are provided in the Supporting Information. In the ^{1}H NMR spectrum of the initial mixture, the amino protons in the aniline unit and the proton at the carbon–carbon triple bond of the alkyne give rise to singlet signals at $\delta = 3.38$ and 2.76 ppm, respectively. The methyl group in **13b** is represented in the ^{1}H NMR spectrum by a resonance at $\delta = 1.78$ ppm. The protons of the H_2N group in **13c** appear in the ^{1}H NMR spectrum at $\delta = 3.79$ ppm and two signals at $\delta = 5.30$ and 5.74 ppm correspond to the two diastereotopic protons at the carbon–carbon double bond.

The course of the reaction of 1-aminoanthracene (**14a**), with phenylacetylene catalyzed by digallane **1** changes to give exclusive formation of the hydroarylation product **14b**, which has been isolated and characterized (including by single-crystal X-ray analysis). Note, insertions of acetylenes into aromatic carbon–hydrogen bonds catalyzed by Rh and Ru complexes have been reported.[25] The crystal data and structure refinement details for compounds **7b** and **14b** are reported in Table 3, their molecular structures are depicted in Figures 11 and 12, respectively. The crystal data confirm the formation of the Markovnikov hydroamination product **7b**. The C–C and C–N bond lengths in **7b** are in the range expected for an organic compound. Restricted rotation around the C(14)–C(15) bond in **14b** causes the existence of two enantiomers.

Notably, the hydroamination of alkynes with anilines described above is relevant in Kutcherov's hydration of acetylenes.[26] We suggest that, similar to alkyne hydration,[27] the amination of alkynes proceeds by nucleophile attack of

Table 2. Reaction of phenylacetylene with anilines, catalyzed by complex **1**.

hydroamination:

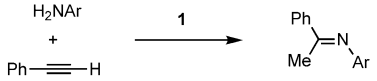

hydroarylation:

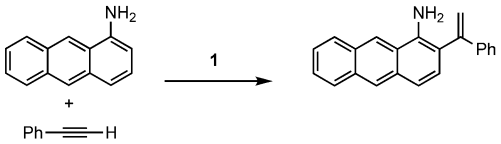

Entry	Aniline		Product		*t* [h]	*T* [°C]	Yield [%]
1	**6a**	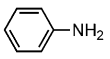	**6b**	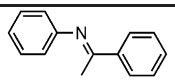	16	90	>99
2	**7a**	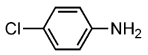	**7b**	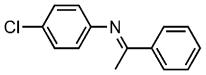	6	110	>99
3	**8a**	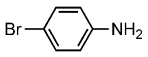	**8b**	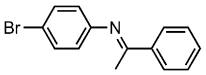	90	110	19
4	**9a**	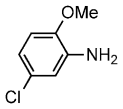	**9b**	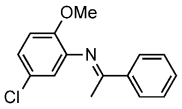	50	110	98
5	**10a**	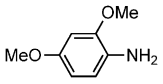	**10b**	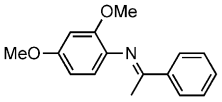	200	110	95
6	**11a**	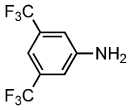	**11b**	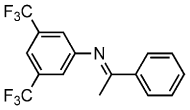	18	110	92
7	**12a**	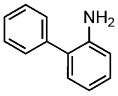	**12b**	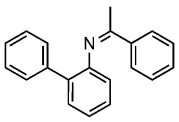	66	90	13
8	**13a**		**13b**	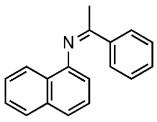	12	90	48
			13c	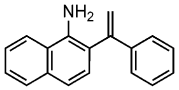			52
9	**14a**	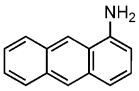	**14b**	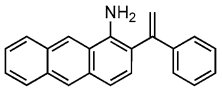	18	90	>99

$ArNH_2$ on the activated/coordinated alkyne. A change of the reaction course from hydroamination (for **6a**<Pr>**6b**) to hydroarylation of phenylacetylene (**13a**<Pr>**13c** and **14a**<Pr>**14b**) leads to the conclusion that, in the series considered, the nucleophilic character of the carbon atom *ortho* to the amino group increases with extension of the π system. Additionally, the nucleophilic character of the *ortho*-carbon atom becomes comparable, or even stronger, than that of the nitrogen atom of the amino group.

Comparison of the catalytic activity of complex **1** with simple gallium compounds, such as Et_3Ga and $GaCl_3$, is quite interesting. In the presence of Et_3Ga (50 mol%), phenylacetylene reacts with 4-chloroaniline (**7a**) to give hydroamination product **7b** in 99% yield within 30 h. Comparatively, with catalyst **1** (2 mol%), compound **7b** can be obtained in quantitative yield after 6 h. Note, in the presence of Et_3Ga (10 mol%) no reaction between PhC≡CH and **7a** could be observed over 50 h at 110°C. For the phenylacetylene/**14a** system two different reaction routes were observed, dependent on whether digallane **1** or $GaCl_3$ was employed as the catalyst (Scheme 4). Under equivalent reaction conditions (C_6D_6, 90°C, 18 h), the amine **14a** and PhC≡CH react catalyzed by **1** (2 mol%) to afford the hydroarylation product **14b** in nearly quantitative yield, whereas these reagents interact under $GaCl_3$ (5.2 mol%) catalysis to give the hydroamination product **14c** in only 55% yield (Scheme 4).

The difference in activity between **1**, Et_3Ga, and $GaCl_3$ as catalysts in the reactions of PhC≡CH with anilines suggests that the kinetically active species generated from these gallium compounds have a different nature and catalyze the reactions by different mechanisms. The most important observation is that a combination of the redox-active dpp-bian ligand with gallium resulted in catalytic systems with much higher efficiency than that of typical Lewis acids. Further, the activity of **1** as a catalyst is comparable to catalysts based on transition metals, for example, [Ir(bispyrazolylemethane)$(CO)_2$][$BArF_4$] (Ar=3,5-bis(trifluoromethyl)phenyl),[28] [(3-iminophosphine)Pd(allyl)][OSO_2CF_3],[29] and $Ti(NMe_2)_4$[30] (Table 4).

We suggest that hydroamination of PhC≡CH with anilines catalyzed by **1** proceeds through attack of the carbon atom at the double bond of the stable intermediate **3** by aniline (Scheme 5), similar to Kutcherov's hydration reaction.

The resulting intermediate **I** undergoes proton transfer to afford intermediate **II**, which is unstable due to its constrain-

Table 3. Crystal data and structure refinement details for compounds **7b** and **14b**.

Compound	**7b**	**14b**
Formula	$C_{14}H_{12}ClN$	$C_{22}H_{17}N$
M_r [g mol^{-1}]	229.70	295.37
T [K]	150	100
crystal system	monoclinic	monoclinic
space group	$P21/n$	P2/1
a [Å]	14.0214(12)	6.2024(3)
b [Å]	13.8297(12)	13.0085(6)
c [Å]	18.1938(15)	9.3124(5)
α [°]	90	90
β [°]	98.143(2)	92.6940(10)
γ [°]	90	90
V [Å^3]	3492.4(5)	750.53(6)
Z	12	2
ρ_{calc}, [g m^{-3}]	1.311	1.307
μ [mm^{-1}]	0.298	0.075
F(000)	1440	312
crystal size [mm^3]	0.37×0.35×0.33	0.38×0.18×0.18
$\theta_{min}/\theta_{max}$	2.08/26.00	2.19/25.98
index ranges	$-17 \le h \le 17$	$-7 \le h \le 7$
	$-12 \le k \le 17$	$-16 \le k \le 15$
	$-22 \le l \le 22$	$-11 \le l \le 8$
reflections collected	19551	4548
independent reflections	6855	2535
R_{int}	0.0489	0.0229
max/min transmission	0.9082/0.8979	0.9865/0.9719
data/restraints/parameters	6855/0/436	2535/1/224
GOF on F^2	0.946	1.040
final R indices [$I>2\sigma(I)$]	$R_1=0.0499$	$R_1=0.0363$
	$wR_2=0.0975$	$wR_2=0.0948$
R indices (all data)	$R_1=0.1064$	$R_1=0.0376$
	$wR_2=0.1116$	$wR_2=0.0960$
largest diff. peak/hole [e Å^{-3}]	0.358/−0.220	0.210/−0.149

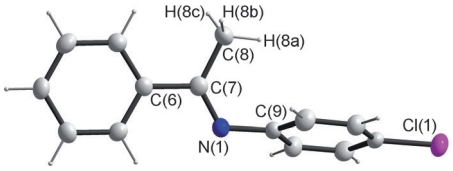

Figure 11. The molecular structure of complex **7b**. Selected bond lengths [Å]: N(1)–C(7) 1.279(3), N(1)–C(9) 1.422(3), C(6)–C(7) 1.491(3), C(7)–C(8) 1.509(3).

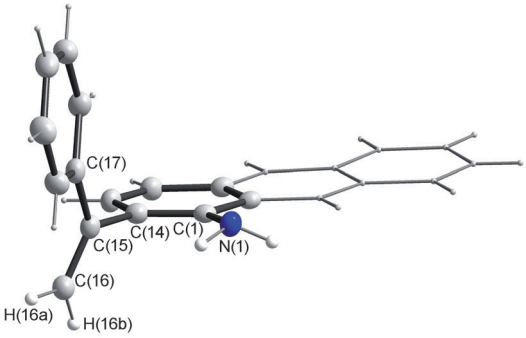

Figure 12. The molecular structure of complex **14b**. Selected bond lengths [Å]: N(1)–C(1) 1.396(2), C(1)–C(14) 1.380(2), C(14)–C(15) 1.501(2), C(15)–C(16) 1.335(2), C(15)–C(17) 1.491(2).

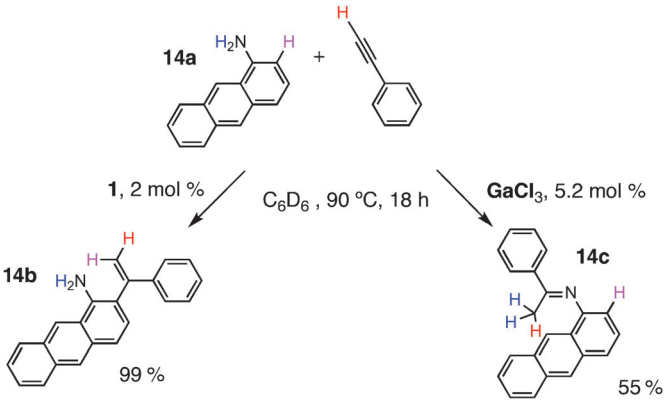

Scheme 4. Comparison of the catalytic activity of digallane **1** and $GaCl_3$ in the reaction of 1-aminoanthracene with phenylacetylene.

Table 4. Comparison of the catalytic activity of digallane **1** with transition-metal complexes in the reaction of PhC≡CH with phenylamine.

Entry	Catalyst	mol %	t [h]	T [°C]	Yield [%]
1	**1**	2	16	90	100
2	$[Ir(bpm)(CO)_2][BArF_4]$[a]	5	22	60	57
3	[(3-IP)Pd(allyl)][OTf][b]	5	22	70	75
4	$Ti(NMe_2)_4$	10	2	75	49

[a] bpm = bispyrazolylmethane, ArF = 3,5-bis(trifluoromethyl)phenyl; [b] 3-IP = 3-iminophosphine, Tf = trifluoromethanesulfonyl.

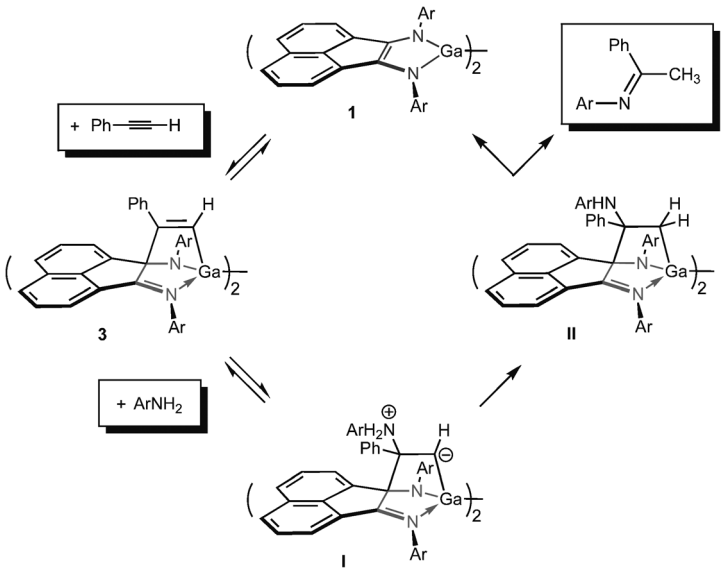

Scheme 5. Hydroamination of phenylacetylene with anilines catalyzed by **1**.

ed structure and weakened C–C and C–Ga bonds. Structure **II** represents the case in which an olefin is added across the Ga–N–C 1,3-dipole but, as discussed above, complex **1** is inert towards olefins and non-alkyne organic substances that contain multiple carbon–carbon and carbon–element bonds. Elimination of the α-aminoolefin regenerates catalyst **1**. The α-aminoolefin isomerizes to afford the final imine product (Scheme 5).

Conclusion

Combining main-group metals with redox-active ligands allows the design of metal complexes with reactivity that resembles that of redox-active transition-metal complexes with redox-inactive spectator ligands. As shown by the reactions of bis-amide gallium complex **1** with a series of alkynes the coordination of π bonds becomes possible by a molecular assembly that comprises of a main-group metal and redox-active ligand. The system (dpp-bian)/gallium is exclusively selective towards alkynes. We believe that addition of an alkyne to complex **1** proceeds as a concerted process that involves the LUMO (π*) of the alkyne and the HOMO (π) of the digallane **1**. However, it is still inexplicable why alkenes, nitriles, ketones, and isonitriles do not react with **1**. We believe the situation can be altered by replacement of the substituents at the nitrogen atoms with stronger electron-donating groups. Variation of the metal may also dramatically influence the reactivity of the dpp-bian dianion. We have already demonstrated that reaction of diallane (dpp-bian)Al–Al(dpp-bian) with PhC≡CH proceeds as 1,3-dipolar cycloaddition but affords a thermally stable regioisomer, in which the phenyl ring is oriented towards the metal. The results of hydroamination/hydroarylation of PhC≡CH with anilines catalyzed by complex **1** are promising. The reaction rates are comparable with other catalytic systems, which include those based on transition metals. We believe that use of co-catalysts or additives can optimize the process. Kinetic experiments will give more insight into the mechanisms of the reactions of alkynes with anilines. We intend to involve other electron-rich substrates, for instance, disulfides, thiols, and phosphines, in the reactions with alkynes in the presence of **1**.

Experimental Section

General remarks: All manipulations were carried out under vacuum by using Schlenk techniques. Diethyl ether, 1,2-dimethoxyethane, THF, benzene, and toluene were condensed into the reaction flask from sodium/benzophenone prior to use. Deuterated solvents [D_8]THF, [D_6]benzene, and [D_8]toluene (Aldrich) were distilled at ambient temperature over sodium/benzophenone and, just prior to use, condensed under vacuum into NMR tubes that contained the compound to be analyzed. NMR spectra were obtained on Bruker DPX 200 and Bruker Avance III spectrometers; arom. = aromatic, d = doublet, m = multiplet, t = triplet, pst = pseudotriplet, s = singlet, sept = septet. UV spectra were recorded on a Perkin–Elmer λ 25 spectrometer. IR spectra (4000–400 cm^{-1}) were obtained on Specord M-80 in Nujol; (vs) very strong, (s) strong, (m) medium, (w) weak. Diimine dpp-bian was prepared according to a literature procedure.[17] Differential scanning calorimetry (DSC) was carried out on a DSC 200 PC (NETZSCH) under nitrogen. Thermal gravimetric analysis (TGA) was carried out on a Pyris 6 TGA under nitrogen at a heating rate of 5 °C min^{-1}. Melting points were determined in sealed capillaries: dec = decomposition. Complex **1** was prepared by reaction of dpp-bian (0.5 g, 1.0 mmol) with gallium metal (4 g, 57 mmol) in toluene (30 mL) at reflux temperature, then used in situ. The yields of **2**–**5** are calculated based on the amount of dpp-bian used for the preparation of **1**.

Compound 2: Acetylene (24 mL, 1.1 mmol) was added to a solution of complex **1** [generated in situ from dpp-bian (0.5 g)] in toluene (30 mL). An immediate color change from deep-blue to red was observed. Toluene was removed under vacuum and the residue was dissolved in Et_2O. Crystallization from Et_2O afforded complex **2** as red crystals (0.43 g, 72 %). M.p. >100 °C (dec); ^{1}H NMR (400 MHz, [D_8]toluene, 25 °C, TMS): δ = 7.96 (d, ^3J = 9.2 Hz, 1H; arom.), 7.33 (d, ^3J = 8.2 Hz, 1H; arom.), 7.24 (d, ^3J = 8.2 Hz, 1H; arom.), 7.22–7.20 (m, 3H; arom.), 7.10–7.08 (m, 3H; arom.), 6.94 (pst, ^3J = 7.6 Hz, 1H; arom.), 6.91 (dd, ^3J = 9.2, 3.1 Hz, 1H; arom.), 6.80 (pst, ^3J = 7.6 Hz, 1H; arom.), 6.61 (d, ^3J = 7.0 Hz, 1H; arom.), 6.45 (d, ^3J = 7.0 Hz, 1H; arom.), 3.78 (sept, ^3J = 6.8 Hz, 1H; C*H*-$(CH_3)_2$), 3.60 (sept, ^3J = 6.8 Hz, 1H; C*H*$(CH_3)_2$), 3.48 (sept, ^3J = 6.8 Hz, 1H; C*H*$(CH_3)_2$), 2.87 (sept, ^3J = 6.8 Hz, 1H; C*H*$(CH_3)_2$), 1.64 (d, ^3J = 6.8 Hz, 3H; CH(C*H*$_3)_2$), 1.25 (d, ^3J = 6.8 Hz, 3H; CH(C*H*$_3)_2$), 1.24 (d, ^3J = 6.8 Hz, 3H; CH(C*H*$_3)_2$), 1.06 (d, ^3J = 6.8 Hz, 3H; CH(C*H*$_3)_2$), 0.83 (d, ^3J = 6.8 Hz, 3H; CH(C*H*$_3)_2$), 0.54 (d, ^3J = 6.8 Hz, 3H; CH(C*H*$_3)_2$), 0.47 (d, ^3J = 6.8 Hz, 3H; CH(C*H*$_3)_2$), −0.03 ppm (d, ^3J = 6.8 Hz, 3H; CH(C*H*$_3)_2$); IR (nujol): $\tilde{\nu}$ = 1640 (vs), 1586 (m), 1360 (s), 1324 (m), 1310 (m), 1274 (m), 1254 (s), 1207 (w), 1187 (m), 1157 (w), 1100 (m), 1058 (w), 1040 (s), 1004 (w), 977 (w), 934 (s), 903 (w), 861 (m), 832 (m), 799 (s), 781 (vs), 754 (s), 715 (s), 644 (w), 617 (w), 603 (w), 578 (w), 545 (w), 521 (w), 497 (w), 462 cm^{-1} (m); elemental analysis calcd (%) for $C_{76}H_{84}Ga_2N_4$ (1192.91): C 76.52, H 7.10; found: C 76.41, H 6.98.

Compound 3: Phenylacetylene (0.1 g, 1.0 mmol) was added to a solution of complex **1** [generated in situ from dpp-bian (0.5 g)] in toluene (30 mL). The mixture turned red immediately. Toluene was removed under vacuum and the residual solid was crystallized from 1,2-dimethoxyethane. Complex **3** was isolated as red crystals (0.52 g, 78 %). M.p. >100 °C (dec); ^{1}H NMR (400 MHz, [D_8]toluene, 25 °C, TMS): δ = 7.93 (s, 1H; *H*(Ga)C=C(C)Ph), 7.38 (d, ^3J = 8.0 Hz, 1H; arom.), 7.24–7.18 (m, 2H; arom.), 7.13 (d, ^3J = 8.0 Hz, 1H; arom.), 7.10–7.06 (m, 3H; arom.), 6.90 (dd, ^3J = 6.5, 2.0 Hz, 1H; arom.), 6.84 (pst, ^3J = 7.8 Hz, 1H; arom.), 6.66 (pst, ^3J = 7.8 Hz, 1H; arom.), 6.61 (pst, ^3J = 7.3 Hz, 1H; arom.), 6.57 (m, 3H; arom.), 6.49 (m, 2H; arom.), 6.38 (d, ^3J = 6.8 Hz, 1H; arom.), 4.28 (sept, ^3J = 6.8 Hz, 1H; C*H*$(CH_3)_2$), 3.65 (sept, ^3J = 6.8 Hz, 1H; C*H*-$(CH_3)_2$), 3.44 (sept, ^3J = 6.8 Hz, 1H; C*H*$(CH_3)_2$), 3.06 (sept, ^3J = 6.8 Hz, 1H; C*H*$(CH_3)_2$), 1.70 (d, ^3J = 6.8 Hz, 3H; CH(C*H*$_3)_2$), 1.39 (d, ^3J = 6.8 Hz, 3H; CH(C*H*$_3)_2$), 1.31 (d, ^3J = 6.8 Hz, 3H; CH(C*H*$_3)_2$), 1.10 (d, ^3J = 6.8 Hz, 3H; CH(C*H*$_3)_2$), 0.88 (d, ^3J = 6.8 Hz, 3H; CH(C*H*$_3)_2$), 0.61 (d, ^3J = 6.8 Hz, 3H; CH(C*H*$_3)_2$), 0.43 (d, ^3J = 6.8 Hz, 3H; CH(C*H*$_3)_2$), −0.12 ppm (d, ^3J = 6.8 Hz, 3H; CH(C*H*$_3)_2$); IR (nujol): $\tilde{\nu}$ = 1631 (s), 1587 (m), 1524 (w), 1485 (m), 1418 (m), 1362 (m), 1323 (w), 1309 (w), 1256 (m), 1208 (w), 1188 (m), 1157 (w), 1143 (w), 1107 (m), 1078 (w), 1041 (m), 1032 (m), 1003 (w), 968 (w), 938 (w), 895 (w), 861 (m), 833 (m), 816 (w), 802 (m), 783 (s), 752 (s), 698 (s), 676 (m), 658 (m), 612 (w), 589 (w), 557 (w), 481 (w), 463 cm^{-1} (w); elemental analysis calcd (%) for $C_{88}H_{92}Ga_2N_4{\cdot}C_4H_{10}O_2$ (1435.27): C 76.99, H 7.16; found: C 76.81, H 7.07.

Compound 4: Methyl-2-butynoate (0.1 g, 1.0 mmol) was added to a solution of **1** (generated in situ from dpp-bian (0.5 g)] in toluene (30 mL). An instant color change from deep-blue to red was observed. The solvent was evaporated under vacuum. Crystallization from benzene afforded complex **4** as red crystals (0.46 g, 65 %). M.p. >150 °C (dec); ^{1}H NMR (200 MHz, [D_8]THF, 25 °C, TMS): δ = 7.97 (d, ^3J = 8.3 Hz, 1H; arom.), 7.71 (d, ^3J = 8.3 Hz, 1H; arom.), 7.40–7.18 (m, 5H; arom.), 7.11 (dd, ^3J = 6.8, 2.0 Hz, 1H; arom.), 6.98 (pst, ^3J = 7.5 Hz, 1H; arom.), 6.71 (d, ^3J = 7.3 Hz, 1H; arom.), 6.18 (d, ^3J = 7.3 Hz, 1H; arom.), 6.14 (d, ^3J = 7.3 Hz, 1H; arom.), 4.69 (sept, ^3J = 6.8 Hz, 1H; C*H*$(CH_3)_2$), 3.24–3.07 (m, 2H; C*H*$(CH_3)_2$), 2.83 (sept, ^3J = 6.8 Hz, 1H; CH$(CH_3)_2$), 1.34 (s, 3H; C*H*$_3$C(C)=C(Ga)CO_2CH_3), 1.15 (d, ^3J = 6.8 Hz, 6H; CH(C*H*$_3)_2$), 0.85 (d, ^3J = 6.8 Hz, 3H; CH(C*H*$_3)_2$), 0.68 (d, ^3J = 6.8 Hz, 3H; CH(C*H*$_3)_2$), 0.62 (d, ^3J = 6.8 Hz, 3H; CH(C*H*$_3)_2$), 0.25 (d, ^3J = 6.8 Hz, 3H; CH(C*H*$_3)_2$), −0.36 ppm (d, ^3J = 6.8 Hz, 3H; CH(C*H*$_3)_2$); IR (nujol): $\tilde{\nu}$ = 1701 (m), 1683 (m), 1638 (m), 1588 (w), 1311 (w), 1269 (w), 1251 (w), 1218 (m), 1185 (w), 1156 (w), 1033 (m), 968 (w), 935 (w), 856 (m), 834 (m), 799 (m), 780 (s), 758 (m), 723 (s), 679 (s), 546 cm^{-1} (w); elemental analysis calcd (%) for $C_{82}H_{92}Ga_2N_4O_4{\cdot}C_6H_6$ (1415.14): C 74.68, H 6.98; found: C 74.50, H 6.91.

Compound 5: Ethyl-2-butynoate (0.11 g, 1 mmol) was added to a solution of complex **1** [generated in situ from dpp-bian (0.5 g)]. The color of the reaction mixture changed rapidly from deep-blue to red. Toluene was re-

moved under vacuum and the residue was dissolved in benzene. Slow evaporation of the solvent under vacuum gave **5** as red crystals (0.54 g, 73%). M.p. >150°C (dec); ^{1}H NMR (200 MHz, [D$_8$]THF, 25°C, TMS): δ=7.94 (d, ^3J=8.3 Hz, 1H; arom.), 7.68 (d, ^3J=8.3 Hz, 1H; arom.), 7.38–7.26 (m, 3H; arom.), 7.21 (d, ^3J=6.6 Hz, 1H; arom.), 7.13 (dd, ^3J=6.3, 2.7 Hz, 1H; arom.), 7.00–6.88 (m, 2H; arom.), 6.68 (pst, ^3J=4.8 Hz, 1H; arom.), 6.26 (d, ^3J=7.0 Hz, 1H; arom.), 6.15 (d, ^3J=7.3 Hz, 1H; arom.), 4.37 (m, 1H; $CH_3C(C)$=C(Ga)$CO_2CH_2CH_3$), 4.20 (m, 1H; $CH_3C(C)$=C(Ga)$CO_2CH_2CH_3$), 3.82 (sept, ^3J=6.8 Hz, 1H; $CH(CH_3)_2$), 3.25 (sept, ^3J=6.8 Hz, 1H; $CH(CH_3)_2$), 3.16 (sept, ^3J=6.8 Hz, 1H; $CH(CH_3)_2$), 2.87 (sept, ^3J=6.8 Hz, 1H; $CH(CH_3)_2$), 1.27 (d, ^3J=6.8 Hz, 6H; $CH(CH_3)_2$), 1.25 (d, ^3J=6.8 Hz, 3H; $CH(CH_3)_2$), 1.25 (s, 3H; $CH_3C(C)$=C(Ga)-$CO_2CH_2CH_3$), 1.17 (m, 3H; $CH_3C(C)$=C(Ga)$CO_2CH_2CH_3$), 1.09 (d, ^3J=6.8 Hz, 3H; $CH(CH_3)_2$), 0.84 (d, ^3J=6.8 Hz, 3H; $CH(CH_3)_2$), 0.77 (d, ^3J=6.8 Hz, 3H; $CH(CH_3)_2$), 0.64 (d, ^3J=6.8 Hz, 3H; $CH(CH_3)_2$), 0.31 (d, ^3J=6.8 Hz, 3H; $CH(CH_3)_2$), −0.34 ppm (d, ^3J=6.8 Hz, 3H; $CH(CH_3)_2$); IR (nujol): $\tilde{\nu}$=1698 (s), 1635 (s), 1585 (m), 1314 (m), 1251 (s), 1227 (s), 1188 (m), 1138 (m), 1108 (w), 1099 (w), 1036 (s), 968 (w), 935 (w), 902 (w), 858 (m), 831 (m), 798 (m), 780 (s), 758 (s), 675 (vs), 592 (w), 547 (m), 525 (w), 489 (m), 463 cm^{-1} (w); elemental analysis calcd (%) for $C_{84}H_{96}Ga_2N_4O_4$·3C_6H_6 (1599.47): C 76.59, H 7.18; found: C 75.15, H 7.22.

Reaction of anilines with phenylacetylene: Phenylacetylene and amines were purchased from Aldrich. 2,4-Dimethoxyaniline was purified by recrystallization from hexane. Liquid amines were distilled from CaH_2. Phenylacetylene was degassed and stored over molecular sieves (4 Å). Samples were prepared in NMR tubes under vacuum by dissolving the catalyst **1** (0.02 mmol), phenylacetylene (1.0 mmol), and amine (1.0 mmol) in [D$_6$]benzene (0.5 mL). The NMR tubes were sealed under vacuum and then placed in a temperature-controlled oil bath (90–110°C). Conversion of the reagents was monitored by ^{1}H NMR spectroscopy. The ratio between the reagents and the product was calculated from the integral intensities of the corresponding signals.

Compound 7b: Complex **1** (0.22 g, 0.2 mmol) was added to a solution of phenylacetylene (1.0 g, 10 mmol) and 4-chloroaniline (1.28 g, 10 mmol) in benzene (30 mL). The color of the solution turned red. The reaction mixture was heated at reflux temperature (110°C) for 6 h and the solution changed color from red to dark-brown. Benzene was removed under vacuum and the residue was dissolved in *n*-hexane. Slow evaporation of the solvent afforded complex **7b** as colorless crystals. ^{1}H NMR (200 MHz, $CDCl_3$, 25°C, TMS): δ=7.96 (m, 2H; arom.), 7.46 (m, 3H; arom.), 7.32 (d, ^3J=8.5 Hz, 2H; arom.), 6.74 (d, ^3J=8.5 Hz, 2H; arom.), 2.24 ppm (s, 3H; N=C(CH_3)Ph); elemental analysis calcd (%) for $C_{14}H_{12}ClN$ (229.70): C 85.33, H 5.22; found: C 84.96, H 5.07.

Compound 14b: Complex **1** (0.22 g, 0.2 mmol) was added to a solution of phenylacetylene (1.0 g, 10 mmol) and 1-aminoanthracene (2.95 g, 10 mmol) in benzene (30 mL). The mixture turned red immediately. The reaction mixture was heated at reflux temperature (90°C) for 18 h and the solution changed color from red to dark-brown. Benzene was removed under vacuum and the residual solid was crystallized from *n*-hexane. Complex **14b** was isolated as colorless crystals. ^{1}H NMR (400 MHz, $CDCl_3$, 25°C, TMS): δ=8.42 (d, ^3J=4.5 Hz, 2H; arom.), 8.02 (dd, ^3J=7.0 Hz, 2H; arom.), 7.50 (m, 5H; arom.), 7.37 (m, 3H; arom.), 7.27 (d, ^3J=8.5 Hz, 1H; arom.), 6.03 (d, ^3J=1.26 Hz, 1H; *H*C=C(Ph)), 5.55 (d, ^3J=1.26 Hz, 1H; *H*C=C(Ph)), 4.42 ppm (s, 2H; NH_2); elemental analysis calcd (%) for $C_{22}H_{17}N$ (295.37): C 89.38, H 5.76; found: C 89.47, H 5.63.

Single-crystal X-ray structure determination of 2–5, 7b, and 14b: The data were collected on a Bruker APEX II CCD diffractometer (**2**–**5**) or a Bruker SMART APEX diffractometer (**7b**, **14b**). In both diffractometers, graphite monochromated Mo$_{K\alpha}$ radiation (ω-scan technique, λ= 0.71073 Å) was used. The structures were solved by direct methods by using SHELXS-97[31] and were refined on F^2 with SHELXL-97.[32] SADABS[33] was used to perform area-detector scaling and absorption corrections. All non-hydrogen atoms were refined anisotropically. The hydrogen atoms were placed in calculated positions and assigned to an isotropic displacement parameter of 0.08 Å^2. CCDC-770785 (**2**), CCDC-770786 (**3**), CCDC-770787 (**4**), CCDC-770788 (**5**), CCDC-836606 (**7b**), and CCDC-836607 (**14b**) contain the supplementary crystallographic data for this paper. These data can be obtained free of charge from The Cambridge Crystallographic Data Centre via www.ccdc.cam.ac.uk/data_request/cif.

Acknowledgements

This work was supported by the Russian Ministry of Education and Science (contract no. 14.740.11.0613), the Russian Foundation for Basic Research (grant no. 11–03–01184), and the Alexander von Humboldt foundation (partnership project between G.A. Razuvaev, Institute of Organometallic Chemistry, and the Technical University of Berlin). The authors thank Prof. K. A. Lyssenko, Dr. A. S. Shavyrin, Mrs. T. I. Lopatina, and Dr. A. V. Arapova for assistance with X-ray analysis, NMR spectroscopy, TGA, and DSC experiments, respectively. We thank Dr. E. C. E. Rosenthal for fruitful discussions.

[1] a) R. van Asselt, E. E. C. G. Gielens, R. E. Rulke, C. J. Elsevier, *J. Chem. Soc. Chem. Commun.* **1993**, 1203–1205; b) R. van Asselt, K. Vrieze, C. J. Elsevier, *J. Organomet. Chem.* **1994**, *480*, 27–40; c) R. van Asselt, C. J. Elsevier, W. J. J. Smeets, A. L. Spek, R. Benedix, *Recl. Trav. Chim. Pays-Bas* **1994**, *113*, 88–98; d) R. van Asselt, C. J. Elsevier, *Organometallics* **1994**, *13*, 1972–1980; e) R. van Asselt, C. J. Elsevier, W. J. J. Smeets, A. L. Spek, *Inorg. Chem.* **1994**, *33*, 1521–1531; f) R. van Asselt, E. Rijnberg, C. J. Elsevier, *Organometallics* **1994**, *13*, 706–720; g) R. van Asselt, E. E. C. G. Gielens, R. E. Rulke, K. Vrieze, C. J. Elsevier, *J. Am. Chem. Soc.* **1994**, *116*, 977–985.

[2] a) V. Rosa, C. I. M. Santos, R. Welter, G. Aullon, C. Lodeiro, T. Aviles, *Inorg. Chem.* **2010**, *49*, 8699–8708; b) M. J. Sgro, D. W. Stephan, *Dalton Trans.* **2010**, *39*, 5786–5794; c) S. I. Pascu, G. Balazs, J. C. Green, M. L. H. Green, I. C. Vei, J. E. Warren, C. Windsor, *Inorg. Chim. Acta* **2010**, *363*, 1157–1172; d) J. Parmene, A. Krivokapic, M. Tilset, *Eur. J. Inorg. Chem.* **2010**, 1381–1394; e) C. Zuccaccia, G. Bellachioma, G. Ciancaleoni, A. Macchioni, D. Zuccaccia, *Inorg. Chim. Acta* **2010**, *363*, 595–600; f) K. M. Clark, J. W. Ziller, A. F. Heyduk, *Inorg. Chem.* **2010**, *49*, 2222–2231; g) T. Kern, U. Monkowius, M. Zabel, G. Knoer, *Eur. J. Inorg. Chem.* **2010**, 4148–4156; h) B. L. Small, R. Rios, E. R. Fernandez, D. L. Gerlach; J. A. Halfen, M. J. Carney, *Organometallics* **2010**, *29*, 6723–6731; J. A. Halfen, M. J. Carney, *Organometallics* **2010**, *29*, 6723–6731; i) S. Park, T. Okada, D. Takeuchi, K. Osakada, *Chem. Eur. J.* **2010**, *16*, 8662–8678; j) C. Chen, R. F. Jordan, *J. Am. Chem. Soc.* **2010**, *132*, 10254–10255; k) C. Chen, S. Luo, R. F. Jordan, *J. Am. Chem. Soc.* **2010**, *132*, 5273–5284; l) Y. Miyamura, K. Kinbara, Y. Yamamoto, V. K. Praveen, K. Kato, M. Takata, A. Takano, Y. Matsushita, E. Lee, M. Lee, T. Aida, *J. Am. Chem. Soc.* **2010**, *132*, 3292–3294.

[3] For a review article on main-group metal complexes of bian ligands, see: N. J. Hill, I. Vargas-Baca, A. H. Cowley, *Dalton Trans.* **2009**, 240–253.

[4] I. L. Fedushkin, A. A. Skatova, V. A. Chudakova, G. K. Fukin, *Angew. Chem.* **2003**, *115*, 3416–3420; *Angew. Chem. Int. Ed.* **2003**, *42*, 3294–3298.

[5] I. L. Fedushkin, V. M. Makarov, V. G. Sokolov, G. K. Fukin, *Dalton Trans.* **2009**, 8047–8053.

[6] a) 120 complexes of bians with Group 1, 2, 13, and 14 metals are reported; b) 22 complexes of bians with lanthanides are reported. For full lists of references see the Supporting Information.

[7] W. I. Dzik, J. I. van der Vlugt, J. N. H. Reek, B. de Bruin, *Angew. Chem.* **2011**, *123*, 3416–3418; *Angew. Chem. Int. Ed.* **2011**, *50*, 3356–3358.

[8] a) I. L. Fedushkin, N. M. Khvoinova, A. A. Skatova, G. K. Fukin, *Angew. Chem.* **2003**, *115*, 5381–5384; *Angew. Chem. Int. Ed.* **2003**, *42*, 5223–5226; b) I. L. Fedushkin, A. A. Skatova, V. K. Cherkasov, V. A. Chudakova, S. Dechert, M. Hummert, H. Schumann, *Chem. Eur. J.* **2003**, *9*, 5778–5783; c) I. L. Fedushkin, A. A. Skatova, A. N. Lukoyanov, V. A. Chudakova, S. Dechert, M. Hummert, H. Schu-

mann, *Russ. Chem. Bull.* **2004**, *53*, 2751–2762; d) I. L. Fedushkin, A. A. Skatova, M. Hummert, H. Schumann, *Eur. J. Inorg. Chem.* **2005**, 1601–1608; e) I. L. Fedushkin, A. G. Morozov, O. V. Rassadin, G. K. Fukin, *Chem. Eur. J.* **2005**, *11*, 5749–5757; f) I. L. Fedushkin, A. A. Skatova, G. K. Fukin, M. Hummert, H. Schumann, *Eur. J. Inorg. Chem.* **2005**, 2332–2338; g) I. L. Fedushkin, A. G. Morozov, V. A. Chudakova, G. K. Fukin, V. K. Cherkasov, *Eur. J. Inorg. Chem.* **2009**, 4995–5003; h) I. L. Fedushkin, A. S. Nikipelov, A. A. Skatova, O. V. Maslova, A. N. Lukoyanov, G. K. Fukin, A. V. Cherkasov, *Eur. J. Inorg. Chem.* **2009**, 3742–3749.

[9] I. L. Fedushkin, A. S. Nikipelov, K. A. Lyssenko, *J. Am. Chem. Soc.* **2010**, *132*, 7874–7875.

[10] R. Siebenlist, H.-W. Frühauf, K. Vrieze, W. J. J. Smeets, A. L. Spek, *Organometallics* **2002**, *21*, 5628–5641.

[11] a) M. van Wijnkoop, P. P. M. de Lange, H.-W. Frühauf, K. Vrieze, W. J. J. Smeets, A. L. Spek, *Organometallics* **1995**, *14*, 4781–4791; b) P. P. M. de Lange, R. P. de Boer, M. van Wijnkoop, J. M. Ernsting, H.-W. Frühauf, K. Vrieze, W. J. J. Smeets, A. L. Spek, K. Goubitz, *Organometallics* **1993**, *12*, 440–453; c) P. P. M. de Lange, E. Alberts, M. van Wijnkoop, H.-W. Frühauf, K. Vrieze, H. Kooijman, A. L. Spek, *J. Organomet. Chem.* **1994**, *465*, 241–249; d) N. Feiken, H.-W. Frühauf, K. Vrieze, J. Fraanje, K. Goubitz, *Organometallics* **1994**, *13*, 2825–2832.

[12] a) J. Scholz, H. Goerls, *Inorg. Chem.* **1996**, *35*, 4378–4382; b) J. Scholz, H. Goerls, H. Schumann, R. Weimann, *Organometallics* **2001**, *20*, 4394–4402.

[13] a) P. Barbaro, C. Bianchini, C. Mealli, A. Meli, *J. Am. Chem. Soc.* **1991**, *113*, 3181–3183; b) S. Dutta, S.-M. Peng, S. Bhattacharya, *Inorg. Chem.* **2000**, *39*, 2231–2234.

[14] a) G. A. Abakumov, A. I. Poddel'sky, E. V. Grunova, V. K. Cherkasov, G. K. Fukin, Y. A. Kurskii, L. G. Abakumova, *Angew. Chem.* **2005**, *117*, 2827–2831; *Angew. Chem. Int. Ed.* **2005**, *44*, 2767–2771; b) G. A. Abakumov, V. K. Cherkasov, E. V. Grunova, A. I. Poddel'skii, L. G. Abakumova, Yu. A. Kurskii, G. K. Fukin, E. V. Baranov, *Dokl. Chem.* **2005**, *405*, 222–225; c) V. K. Cherkasov, G. A. Abakumov, E. V. Grunova, A. I. Poddel'sky, G. K. Fukin, E. V. Baranov, Y. V. Kurskii, L. G. Abakumova, *Chem. Eur. J.* **2006**, *12*, 3916–3927.

[15] I. L. Fedushkin, V. M. Makarov, E. C. E. Rosenthal, G. K. Fukin, *Eur. J. Inorg. Chem.* **2006**, 827–832.

[16] a) Y. Peng, B. D. Ellis, X. Wang, J. C. Fettinger, P. P. Power, *Science* **2009**, *325*, 1668–1670; b) M. A. Dureen, D. W. Stephan, *J. Am. Chem. Soc.* **2009**, *131*, 8396–8397; c) C. Jiang, O. Blacque, H. Berke, *Organometallics* **2010**, *29*, 125–133; d) C. Appelt, H. Westenberg, F. Bertini, A. W. Ehlers, J. C. Slootweg, K. Lammertsma, W. Uhl, *Angew. Chem.* **2011**, *123*, 4011–4014; *Angew. Chem. Int. Ed.* **2011**, *50*, 3925–3928.

[17] A. A. Paulovicova, U. El-Ayaan, K. Shibayama, T. Morita, Y. Fukuda, *Eur. J. Inorg. Chem.* **2001**, 2641–2646.

[18] I. L. Fedushkin, A. N. Lukoyanov, S. Y. Ketkov, M. Hummert, H. Schumann, *Chem. Eur. J.* **2007**, *13*, 7050–7056.

[19] a) R. D. Culp, A. H. Cowley, A. Decken, R. A. Jones, M. R. Bond, L. M. Mokry, C. J. Carrano, *Inorg. Chem.* **1997**, *36*, 5165–5172; b) W. Uhl, H. R. Bock, F. Breher, M. Claesener, S. Haddadpour, B. Jasper, A. Hepp, *Organometallics* **2007**, *26*, 2363–2369.

[20] *Catalytic Heterofunctionalization* (Eds.: A. Togni, H. Grützmacher), Wiley-VCH; Weinheim, **2001**, pp. 91–133.

[21] T. E. Müller, K. C. HultzscH; M. Yus, F. Foubelo, M. Tada, *Chem. Rev.* **2008**, *108*, 3795–3892.

[22] a) I. Aillaud, J. Collin, C. Duhayon, R. Guillot, D. Lyubov, E. Schulz, A. Trifonov, *Chem. Eur. J.* **2008**, *14*, 2189–2200; b) G. Zi, L. Xiang, H. Song, *Organometallics* **2008**, *27*, 1242–1246.

[23] M. R. Crimmin, M. ArrowsmitH; A. G. M. Barrett, I. J. Casely, M. S. Hill, P. A. Procopiou, *J. Am. Chem. Soc.* **2009**, *131*, 9670–9685; A. G. M. Barrett, I. J. Casely, M. S. Hill, P. A. Procopiou, *J. Am. Chem. Soc.* **2009**, *131*, 9670–9685.

[24] a) J. Jenter, R. Köppe, P. W. Roesky, *Organometallics* **2011**, *30*, 1404–1413; b) S. Datta, P. W. Roesky, S. Blechert, *Organometallics* **2007**, *26*, 4392–4394.

[25] a) W. T. Boese, A. S. Goldman, *Organometallics* **1991**, *10*, 782–786; b) U. R. Aulwurm, J. U. Melchinger, H. Kisch; *Organometallics* **1995**, *14*, 3385–3395.

[26] M. G. Kutscheroff, *Ber. Dtsch. Chem. Ges.* **1881**, *14*, 1540–1542.

[27] *March's Advanced Organic Chemistry*, 5th ed. (Eds.: M. B. Smith; J. March), Wiley-VCH; New York, **2001**, p. 995.

[28] S. L. Dabb, B. A. Messerle, *Dalton Trans.* **2008**, 6368–6371.

[29] A. R. Shaffer, J. A. R. Schmidt, *Organometallics* **2008**, *27*, 1259–1266.

[30] Y. Shi, J. T. Ciszewski, A. L. Odom, *Organometallics* **2002**, *21*, 5148.

[31] G. M. Sheldrick, *SHELXS-97 Program for the Solution of Crystal Structures*, Universität Göttingen, Göttingen (Germany), **1990**.

[32] G. M. Sheldrick, *SHELXL-97 Program for the Refinement of Crystal Structures*, Universität Göttingen, Göttingen (Germany), **1997**.

[33] G. M. Sheldrick, SADABS *Bruker/Siemens Area Detector Absorption Correction Program*, Madison, WI (USA), **1998**.

Received: July 21, 2011
Published online: December 2, 2011

